Eric Du

Lab 4 Quantum Interference and Entanglement

Header styling inspired by CS 70: https://www.eecs70.org/

Abstract

In this experiment, we explore the phenomenon of quantum entanglement, and use its properties to violate the CHSH inequality, a historical result to definitively disprove the existence of hidden variable theories. The entanglement process is achieved using two beta barium borate (BBO) crystals, then vary the measurement basis using a series of half wave plates. Using a particular set of measurement bases, we are able to calculate a quantity S, which is bounded above by $|S| \leq 2$ if hidden variable theories exist. The violation of this inequality in our experiment confirms the lack of such theories, and confirms the nonlocal nature of quantum mechanics.

1 Introduction

This report concerns the QIE experiment in the Physics 111B Experimentation Laboratory. In this report, we will begin by detailing the theoretical background for the phenomena, then analyze the data we collect to verify our theoretical results.

2 Theory

In this section, we will go over all the requisite theory needed to complete this lab. First, we will briefly go over quantum states, measurement, and the CHSH inequality, which is the central focus of our experiment.

2.1 Quantum States

In quantum mechanics, the fundamental building block we use to characterize particles is the *quantum state* $|\psi\rangle$. For the purposes of our experiment, we will deal only with two-state systems, meaning that our state $|\psi\rangle$ only has two possible representations fundamentally, those being $|0\rangle$ and $|1\rangle$, or in our case, we will use $|v\rangle$ and $|h\rangle$ for reasons which will become obvious later.

One key property of quantum states, that are different than classical ones is that they need not exist purely in $|v\rangle$ or $|h\rangle$, but may exist in a *linear combination* of these two states. That is, it is possible to find a particle in the state:

$$|\psi\rangle = \alpha\,|v\rangle + \beta\,|h\rangle$$

In this representation, the coefficients $\alpha, \beta \in \mathbb{C}$ represent the measurement probabilities – that is, if we were to measure the state $|\psi\rangle$, the postulates of quantum mechanics says that the state now collapses into one of $|v\rangle$ and $|h\rangle$ (its constituent states), and the probability of either event occurring is given by $|\alpha|^2$ and $|\beta|^2$, respectively.

The theory we've just described is complete for a single particle two-state system. In this lab, we will be dealing with two particles, so it will be useful to investigate how those states behave as well. When we have two non-interacting particles, due to the fact that one particle doesn't affect the other, then intuitively one expects that the behavior of one particle doesn't affect the other. From a probability theory standpoint, we call these two *independent*. As with independent events, if we are to consider the joint probability distribution of two particles, then due to independence it means that the joint probability is just the product of the two probabilities. Because states are inherently vectors, then this definition changes from a simple product to a *tensor product*, which is basically a fancy product symbol. We don't really need to worry too much about it. In essence, a two-particle state can be written as follows:

$$|\psi\rangle = \alpha\,|vh\rangle + \beta\,|hh\rangle \tag{1}$$

where the way we read this is the exact same as the one-particle state: the probability of observing state $|vh\rangle$ is $|\alpha|^2$, and likewise for $|\beta|^2$. The state $|vh\rangle$ is really shorthand for $|v\rangle \otimes |h\rangle$, and this means that the first particle is in the $|v\rangle$ state and the second is in $|h\rangle$.

2.2 Entangled States

We now move on to discussing entangled states. These states, unlike the previous state we explored (state **??**), have the property that they *cannot* be written as an outer product of individual states. In other words, there is no way to write these states as a product state. In particular, we can see that state **??** can be rewritten as:

$$|\psi\rangle = (\alpha |v\rangle_1 + \beta |h\rangle_1) \otimes |h\rangle_2$$

which is indeed a product state. The subscripts are not needed here, but they are added in because it's easier to refer to which particle each state is representing. With two particles, there are four possible entangled states, called the *Bell states*:

$$|\Phi^{\pm}\rangle = \frac{|vv\rangle \pm |hh\rangle}{\sqrt{2}} \quad |\Psi^{\pm}\rangle = \frac{|hv\rangle \pm |vh\rangle}{\sqrt{2}} \tag{2}$$

These states, because they cannot be written as a product state, have the special property that measuring one of the two states immediately tells you the other. For instance, in the ϕ^+ state, measuring the first particle as $|v\rangle$ immediately tells you that the second one is $|h\rangle$, despite having not measured the second particle. Bell states are incredibly important to this lab, so it is imperative that we fully understand them.

2.3 Measurement

One thing we've briefly talked about so far but haven't formalized is the idea of measurement. In our case, a measurement just means projecting state by its a dual vector. For instance, suppose we have the following state $|\psi\rangle$:

$$|\psi\rangle = \cos\theta |v\rangle + \sin\theta |h\rangle \tag{3}$$

Because this is a single particle state, it's easy to just read off the probability of measuring $|v\rangle$ is just $\cos^2\theta$, since that's the magnitude squared of the coefficient of $|v\rangle$. More formally, however, what we are actually doing here is taking the inner product between $|v\rangle$ and $|\psi\rangle$, so the following is what we are actually doing:

$$|\langle v| (\cos\theta |v\rangle + \sin\theta |h\rangle)|^2 = \left|\cos\theta \langle v|v\rangle + \sin\theta \underbrace{\langle v|h\rangle}_{0}\right|^2 = \cos^2\theta$$

To arrive at this result, we also need to assume the following: that $|v\rangle$ and $|h\rangle$ are a set of orthonormal basis vectors. Here, we can assume this is the case, because the polarization direction is simply a unit vector pointing in the direction of polarization, and vertical and horizontal lines are indeed orthogonal to each other. It's easy to see why not having orthonormality kills this condition, since we won't have $\langle v|v\rangle = 1$ and $\langle v|h\rangle = 0$ as we do in the equation above. In the case of two particles, the result isn't that much more interesting, suppose we want to measure $|vv\rangle$ on state $|\Phi^+\rangle$:

$$|\psi\rangle = \langle vv| \left(\frac{|vv\rangle + |hh\rangle}{\sqrt{2}}\right) = \left|\frac{1}{\sqrt{2}} \langle vv|vv\rangle + \frac{1}{\sqrt{2}} \underbrace{\langle vv|hh\rangle}_{0}\right|^2 = \frac{1}{2}$$

so just like how $\langle v|h\rangle = 0$, we also have $\langle vv|hh\rangle = 0$, nothing major changes. In our experiment, we will be dealing with different measurement bases, given by our half wave plates (HWPs) which we will talk about later. Therefore, we will not always be measuring in the $|v\rangle$ basis; in fact most of the time we won't be measuring in such a basis. Instead, we will measure in a rotated basis, where the first and second photon will be rotated by some arbitrary angles α and β counterclockwise away from the vertical. The math doesn't change, but the equation is a bit more rich now, since we need to capture the rotation. Let

$M(\alpha, \beta)$ denote the measurement projection. Given the rotation angles, we can write down the new basis in terms of the old $\{v, h\}$ basis as:

$$M(\alpha, \beta) = (\cos\alpha \langle v| + \sin\alpha \langle h|) \otimes (\cos\beta \langle v| + \sin\beta \langle h|) \tag{4}$$

Here, the $\langle v|$ and $\langle h|$ are understood to be the corresponding dual vectors to $|v\rangle$ and $|h\rangle$. Thus, to calculate the probability of measuring $|vv\rangle$ in the new basis, we can take the inner product of $M(\alpha, \beta)$ with our state to find the probability. For example, we can show that using equation 4 and a bell state, we get:

$$P_{vv}(\alpha, \beta) = \frac{1}{2}|\sin\alpha \sin\beta + \cos\alpha \cos\beta|^2 = \frac{1}{2}\cos^2(\alpha - \beta)$$

[1]. Here, the P_{vv} is used to denote the fact that we are measuring $|vv\rangle$ in the *new* basis, after rotation.

2.4 Hidden Variable Theories, CHSH Inequality

In the 20th century, when the groundwork for quantum mechanics was being laid out, the existence of entangled states like the Bell states troubled researchers, as the idea that measuring the state of one particle determines the state of another regardless of their distance apart seemed ridiculous; in particular, it violated the principle of causality – the principle that no information can travel faster than light, and that everything must be causally related. The solution, in their minds, was to introduce *hidden variable theories*, which postulate the existence of "hidden variables" that cannot be observed, but in some way predetermine the measurement so as to not violate causality.

Some decades later, John Bell proposes an experiment that will help definitively prove whether such hidden variables actually exist. In his work, he effectively proved that for hidden variables to exist, then there exists a calculable bound that must be satisfied, and is violated by quantum mechanics. We won't go into the derivation of the inequality itself which is quite lengthy, but the equation we will be concerned with first concerns a quantity E:

$$E = \frac{N_{vv} + N_{vh} - N_{hv} + N_{hh}}{N_{\text{total}}}$$

Here, N_{vv} characterizes the number of times times the photons are measured to be vertically polarized, and the same goes for the other quantities. N_{total} just refers to the total count. Now, we define a second quantity S, which is at the heart of this inequality:

$$S = E(\alpha, \beta) - E(\alpha, \beta') + E(\alpha', \beta) + E(\alpha', \beta') \leq 2 \tag{5}$$

This is the famous CHSH inequality, which is at the heart of Bell's theorem. According to the theorem, classical hidden variable theories must have an upper bound of $S \leq 2$, whereas such a bound is violated under quantum theories. In essence, what Bell proved is that if we can experimentally show the violation of this bound, then we can definitively rule out hidden variable theories altogether. Such a violation is precisely what awarded John Clauser, Alain Aspect and Anton Zeilinger the Nobel prize in 2022, which shows the degree of importance this equation holds to our faith in quantum mechanics. Our goal in this experiment is to replicate their work and violate this inequality as well.

2.5 Half Wave Plates

One particular element in our optical setup that we will make extensive use of is the half wave plate (HWP). The half wave plate is a piece of birefringent material that changes the polarization of the incoming wave, depending on its polarization. To understand their physics, we follow [2]. Formally, we can say that birefringent materials have a fast and slow axis, whose indices of refraction are n_F and n_s, which tells us how a polarized wave along either axis will behave when it passes through the material. For us, these axes will be $|v\rangle$ and $|h\rangle$. If we write the incoming EM wave as E_1, then we can write the output as:

$$E_2 = s(s \cdot E_1)e^{i\phi_s} + f(f \cdot E_1)e^{i\phi_f}$$

Here, ϕ_s and ϕ_f are the phase shifts incurred by the component of the wave which passes through the fast and slow axis. We can then alter this equation a bit and write it as a single phase shift:

$$E_2 = s(s \cdot E_1)e^{i\phi} + f(f \cdot E_1)$$

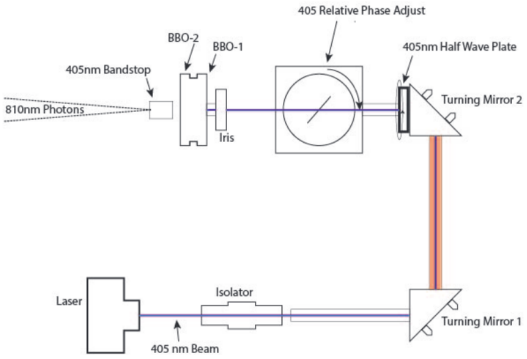

(a)

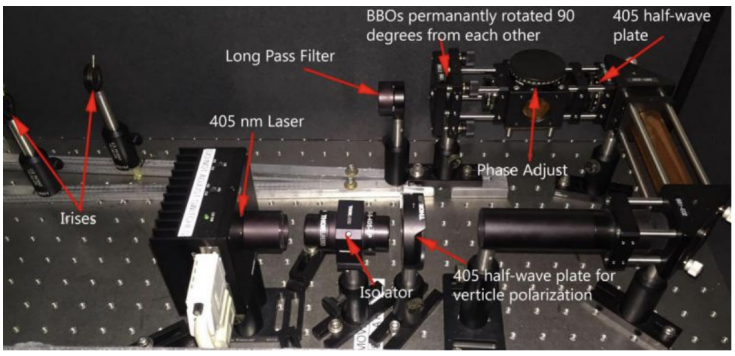

(b)

Figure 1: (a) Schematic diagram of the laser used in the experiment, along with the HWP and BBOs. The 405 nm bandstop is not present in our experiment. (b) Image of the laser as it exists in our experimental setup. The long pass filter and irises were not used in our experiment. Both of these images were taken from [3]

where now, $\phi = \phi_s - \phi_f$. In this formulation, this essentially says that the HWP alters the polarization along the slow axis, but leaves the wave along the fast axis unchanged. In the language that we will use, this effectively means that given a state $|\psi\rangle$ as in 3, the wave plate performs the following transformation:

$$|\psi\rangle \rightarrow |\psi'\rangle = \cos\theta\,|v\rangle + e^{i\phi}\sin\theta\,|h\rangle$$

A half wave plate has exactly $\phi = \pi$, so here $|\psi'\rangle = \cos\theta\,|v\rangle - \sin\theta\,|h\rangle$. This is equivalent to a rotation by 2θ – we can see this because subtacting 2θ from $|\psi'\rangle$, we obtain:

$$\cos(\theta - 2\theta)\,|v\rangle - \sin(\theta - 2\theta)\,|h\rangle = \cos(-\theta)\,|v\rangle - \sin(-\theta)\,|h\rangle = \cos(\theta)\,|v\rangle + \sin\theta\,|h\rangle = |\psi\rangle$$

and so subtracting by 2θ does recover the original state $|\psi\rangle$, confirming the fact that a HWP rotates by 2θ. This will be extremely important in this lab, as we make use of multiple HWPs throughout the experiment.

3 Experimental Setup

Our experimental setup is split into two parts, the laser and the detector. Save for a few dials, the laser portion of the apparatus will remain untouched for the majority of the experiment, but it is nevertheless important to understand the physics of it anyways. Figure 1a shows a schematic diagram of the laser setup. As shown in the figure, a 405 nm beam of violet light is produced by the laser at the bottom, and a linear polarizer (not shown) is placed immediately in front of it so that the violet laser only produces horizontally polarized light. The light then passes through an isolator, through two mirrors and through a HWP. Then, the light passes through a phase adjuster, then into two BBO (beta barium borate) crystals. These crystals are the material that will help us generate the entangled pairs, which we will explain in the next section.

A photo of the detector setup is shown in figure 2, the detector portion of the apparatus consists of two detection arms, with each arm having a HWP, a beam splitter, a long pass filter and a detector at the very end. The beam splitter is a clear cube which only lets through horizontally polarized light, and the long pass filter is used to only allow the entangled photons through, this will also become clear in the next section. The signal from the detectors is then fed through to an APD, a device which measures coincidences (these are the N_{vv} quantities from the earlier section). In this experiment, the coincidences are measured as photons which arrive at both detectors within 5 nanoseconds of each other – for most photons which arrive within this window, we can safely say that they originated from the same photon (before being split by the BBO), and thus are entangled. The size of 5 ns is chosen to account for slight differences in the beam paths and other potential sources of error.

The signal from the APDs is then fed to an FPGA, which is already pre-programmed to send the correct data to the LabVIEW application on the neighboring computer. From here, we can read off the values displayed on the monitor to collect our data.

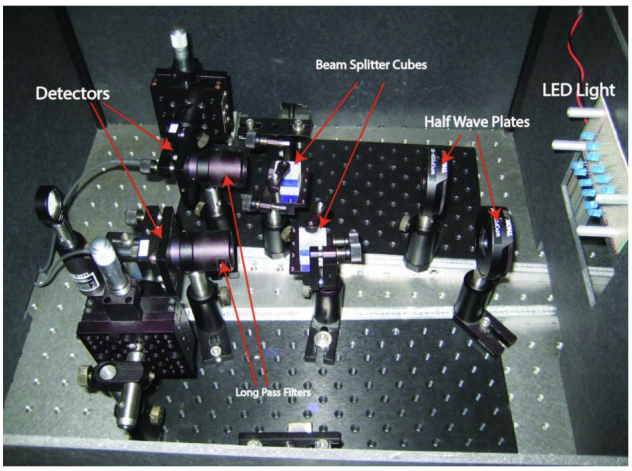

Figure 2: Photo of the detector setup in our experiment. The laser beam comes in from the right, and interacts with the half wave plates, then the beam splitter cubes, before passing through the long pass filter then into the detector. This image was taken from [3]

4 Procedure

For the experimental procedure, we will split this section into multiple parts. The actual experiment itself and the data collection is very easy – all we will have to do is turn the HWPs to specific angles, turn on the laser, and read off the coincidences measured by the detector. Thus, a large part of this section will be dedicated to the *calibration* of the setup, a process that occupied the vast majority of our time.

4.1 Beam Alignment

4.1.1 Violet Beam

To begin, the first section we work on is the first half of the apparatus, where the violet laser light is generated. Here, the first thing we need to make sure above all else is that the entangled pairs of photons are being generated properly. For us, that means we need to verify three things: first, the laser light is properly polarized before entering the HWP. Secondly, that the HWP angle is set to the correct angle to get an even distribution of vertical and horizontal pairs and finally, we need the entire beam path to be level, between the laser and detector. The first criterion is easy to verify: right after the laser passes through the linear polarizer, we use another piece of polarizing film to ensure that the beam is indeed polarized, which we do by rotating the film about the axis of light propagation. To explain how to calibrate the second criterion, it is first useful to understand the BBO plates and how they are set up.

As shown in figure 1a and 1b, there are two BBOs in our experimental setup, one vertical and one horizontal. The objective of the BBOs, as we mentioned earlier, is used to generate the entangled pairs, which is done by "splitting" a photon into two lower energy photons, but ones which have the same polarization as the original incoming photon. That is, the BBOs effectively give us this mapping:

$$|V\rangle \rightarrow |vv\rangle$$

Here, $|V\rangle$ is used to denote a higher energy particle, and $|vv\rangle$ is the two lower energy photons also with vertical polarization. Then, we can rotate one of the BBOs by $90°$, so that we can also generate the horizontal photons:

$$|H\rangle \rightarrow |hh\rangle$$

Now, we can see why we needed the long pass filter on the detector end: because the entangled pairs are only present at lower energy, then in order to ensure that no other particles are being detected we remove them using the long pass filter.

Furthermore, now that we know how the BBOs work, we can move on to the second calibration criterion. Recalling that we ultimately want to create a Bell state after the BBOs, it means that we require an equal portion of $|vv\rangle$ and $|hh\rangle$ pairs after the particles pass through the BBOs – the only way to guarantee that is if we have an equal superposition of $|V\rangle$ and $|H\rangle$, so this motivates us to set the HWP to exactly 22.5° so that we get a rotation of exactly 45°, which gives us the state:

$$|\psi\rangle = \frac{1}{\sqrt{2}}(\,|vv\rangle + |hh\rangle) = |\Phi^+\rangle$$

as an output, which is exactly what we want. Finally, because there is a gap between the two BBOs, we introduce a small phase shift δ to account for this:

$$|\psi\rangle = \frac{1}{\sqrt{2}}(\,|vv\rangle + e^{i\delta}\,|hh\rangle) \tag{6}$$

Finally, the last criterion is also relatively easy: there is a paper target mounted on the detector side of the experiment, so all we had to do was adjust the height of the laser until the light hit the center of the target. This step was actually complete when we found the experiment, so we didn't have to change anything for this portion.

4.1.2 Detector

Now, with the violet beam calibrated, we now move to calibrating the detector half of the experiment. Assuming that we made sure that the laser and detector reside on the same plane, the next thing to make sure is that the detectors are pointed directly at the output of the BBOs, so that the coincidences may be counted.

For this portion, we first took out the HWP, the beam splitter cubes and also the long pass filters. Then, to determine the beam path, we used a red laser and fed it optical fiber, so that the laser light would shine backwards toward the laser. This way, we can see the beam path more easily. We then use the adjusting knobs on the detectors to control the azimuthal and longitudinal angles, and the angle of the beam (we can adjust the detector arm altogether). Therefore, with all these degrees of freedom, it was much harder to find the perfect configuration than it actually seems.

When we had a configuration we thought was good enough, the way we tested it was to power on the laser, and look for the counts on the left side of the LabVIEW program. To do this, we had to place the long-pass filters back to cover the detectors, to protect them against the violet light. Because the long pass filters only filter out frequency (and leave polarization alone), we don't have to be *too* careful with how we place these, so long as we don't touch any other part of the apparatus with it. If the raw counts were high on both arms (about 70,000 is what we aim for), then the detector was calibrated properly.

4.2 Calibration

Now that the entire apparatus is aligned, the next thing we need to do is calibrate the HWPs, both the one in the box with the laser and the two in the box with the detector. Starting with the former, recall that we want this HWP to be rotated to exactly 22.5° so that we get a state which is polarized at exactly 45° before it passes through the BBOs. However, the fundamental issue with simply using the tick marks on the HWP is that it is not reliable, in the sense that a 0° reading on the HWP does not correspond to the vertical. As such, we need another way to determine the optimal HWP angle, where we will make use of the LabVIEW program. To do so, we remove the two HWPs in the detector box, but leave the beam splitting cubes in. Then, we turn on the laser, and turn the HWP until our coincidence counts are maximized. Because the horizontal counts are maximized, this means that in its current configuration the laser is only outputting horizontally polarized light. Then, while we cannot trust the absolute reading, we will assume that the spacing between the tick marks can be trusted, so a rotation by θ can be measured.

To check that we can trust the tick spacing, we can rotate the HWP by 45 degrees, corresponding to a rotation of 90° meaning that the laser now only outputs $|vv\rangle$ states. Such a state is guaranteed to be deflected by the beam splitter, and as a result we should get a coincidence count of near zero. When we attempted this on our HWP, this is precisely what we see. Now, returning to the angle which maximized the coincidence, we now proceed to turn the phase adjustment knob until the counts are maximized; if the coincidences were not already maximized, this process should increase the coincidence counts even further. This configuration for the HWP and phase adjustment were then recorded: the HWP's maximum was found at $27^\circ \pm 2^\circ$, and

θ_A	**Beam A counts**	θ_B	**Beam B counts**
0.5	65042	-65	64426
20	42360	-60	63434
40	7738	-40	31400
60	17432	-20	4806
80	56312	0	25706
100	60688	20	59530
120	23176	40	52033
140	5720	60	14239
160	38100	80	9355
180	66370	100	44214

(a)

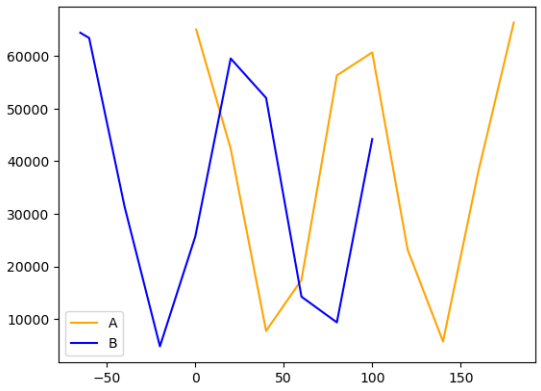

(b)

Figure 3: (a) Table showing the counts for measurement beams A and B. (b) Plot of the count as a function of the angle $\theta_{A,B}$. Linearly interpolating the lines was only done here for visual clarity only, so that we may see the sinusoidal pattern.

the phase was maximized at $308° \pm 2°$. The uncertainty here is determined by the smallest difference between two ticks, which was 2 degrees in both knobs.

Finally, the last thing to calibrate is the half wave plates in the detector box. Before we determining the offsets, it is useful to first verify that the HWPs on both detector arms work as we expect. To verify this, we turn the laser on, and rotate each HWP through a range of angles, recording their *raw counts* (not coincidence counts) periodically. The raw counts are independently calculated for each HWP, so rotating one HWP should not affect the raw count of the other. Because HWPs generate rotations and our measurements are projections, rotating the HWP through a range of angles and observing the raw counts amounts to rotating a vector around the unit circle and observe its projection on the x-axis – essentially, we expect to observe a sinusoid curve. The data for portion and corresponding plot are shown in 3a and 3b, respectively. From the plot, it is clear that a sinusoid is exactly what we observe, which gives good evidence that our HWPs operate as we expect.

Now, we calibrate the HWPs and determine their offset. To do this, we use the configuration derived from the previous paragraph that maximized the counts, and now adjust the HWPs on both arms until we recover the maximum coincidence count. In doing so, we are effectively finding the points on the HWP that are aligned with the $|hh\rangle$ basis – mathematically, this is justified by the principle that the inner product is maximized when the two vectors are collinear, which is what we have here. We can then double check this is indeed the correct orientation, by rotating one of the HWPs by an additional $45°$. Doing so, this changes the measurement basis to the $|hv\rangle$ basis, and as a result we should expect near zero counts – this is precisely what we observe. We then recorded the offsets by reading the angle listed on the HWP at this maximum, which was $295°$ for detector A and $1°$ for detector B.

4.3 Contrast

In this section, we will calculate a quantity called the contrast, which will allow us to essentially determine how ideal our current calibration has been. To do this, we calculate a quantity called the contrast, defined as follows:

$$\text{contrast} = \frac{\max(\text{coincidences}) - \min(\text{coincidences})}{\max(\text{coincidences}) + \min(\text{coincidences})}$$

In an ideal world, we should expect this value to equal 1. This is because the minimum count should be given when our measurement basis is $|hv\rangle$ or $|vh\rangle$, a measurement basis which matches neither of the two states we produce, $|vv\rangle$ and $|hh\rangle$, and as such we should get a coincidence count of zero. We can then compute a contrast for each HWP, by fixing one while varying the other. Doing so, we get a value of 0.987 for detector A, and 0.978 for detector B. The reason they are not exactly 1 is due to experimental uncertainties, with one large contributor likely being the fact despite the room being dark we still obtain

accidental coincidences. However, the fact that they are extremely close to 1 gives good evidence that our half wave plates not only work as expected but the calibration of our system is indeed very good.

5 Results and Analysis

5.1 Characterizing the Bell State

With the HWP contrast calculated, this concludes the last of our calibration, and we now move on to characterizing the Bell state we have produced. To do this, we follow the analysis steps in [1] closely. Recall that if our HWP on the laser side acts as intended, then we produce the state given by equation 6. In general however, because the HWP just generates a rotation, we can write the state after leaving the BBOs as:

$$|\psi_{DC}\rangle = \sin\theta\,|hh\rangle + e^{i\delta}\cos\theta\,|vv\rangle$$

where we rotated by an arbitrary amount θ, measured from the vertical. Our goal is to solve for the value of θ and the phase δ. Given the state above, we can take its inner product with $M(\alpha,\beta)$ from equation 4, which will yield the following probability:

$$\begin{aligned}
P_{vv}(\alpha,\beta) &= |\sin\alpha\sin\beta\cos\theta + e^{i\delta}\cos\alpha\cos\beta\sin\theta|^2 \\
&= \sin^2\alpha\sin^2\beta\cos^2\beta + 2\sin\alpha\sin\beta\cos\theta e^{i\delta}\cos\alpha\cos\beta\sin\theta + \cos^2\alpha\cos^2\beta\sin^2\theta \\
&= \sin^2\alpha\sin^2\beta\cos^2\beta + \cos^2\alpha\cos^2\beta\sin^2\theta + \frac{1}{4}\sin(2\theta)\sin(2\alpha)\sin(2\beta)\cos\delta
\end{aligned}$$

we arrive at the last equation by taking the real part of $e^{i\delta}$, probability is a real quantity. Now, we can then convert this probability into a count:

$$N(\alpha,\beta) = AP_{vv}(\alpha,\beta) + C \tag{7}$$

Here, the value of C exists in order to account for the number of accidental counts we will encounter in our experiment, and A refers to the total number of entangled pairs we generate. This equation should make sense, since $N(\alpha,\beta)$ calculates the expected (in the probabilistic sense) number of coincidences we should get. Now, [1] gives us the following relations:

$$\begin{aligned}
C &= N(0^\circ, 90^\circ) \\
A &= N(0^\circ, 0^\circ) + N(90^\circ, 90^\circ) - 2C
\end{aligned}$$

We can experimentally determine the counts, so we can determine C and A through experiment. Then, going back to equation 7, we can now use the experimentally determined values for A and C to solve for θ and δ, using the following relations:

$$\begin{aligned}
\tan^2\theta &= \frac{N(90^\circ, 90^\circ) - C}{N(0^\circ, 0^\circ - C} \\
\cos\delta &= \frac{1}{\sin(2\theta)}\left(\frac{4(N(45^\circ, 45^\circ) - C}{A} - 1\right)
\end{aligned}$$

We then perform these measurements, which are summarized in table [1]. For each value of N, we took 9 measurements, then computed the arithmetic mean to obtain a value for each $N(\alpha,\beta)$. Then, solving for θ and δ, we obtain:

$$\theta = 43.6^\circ \pm 2^\circ \quad \delta = 37.5 \pm 2^\circ$$

Here, we attach an error of 2° to account for our uncertainty in the setting of our HWPs. In some sense, this is a more natural uncertainty to take than the propagated uncertainty, as it is a better representation of the potential variance in our measurements. This leads to the state:

$$|\psi_{DC}\rangle = 0.72\,|hh\rangle + e^{i\delta}(0.68)\,|vv\rangle$$

Knowing that in the ideal case we have $\theta = 45^\circ$, our experimental value of $\theta = 43.6^\circ$ indicates that our bell state is very nearly ideal (if not exactly ideal), indicating that our calibration steps were done properly. The counts we observe here also

$N(0°, 0°)$	$N(45°, 45°)$	$N(90°, 90°)$	$N(0°, 90°)$
1464	1248	1324	18
1392	1280	1378	12
1480	1324	1252	24
1552	1234	1414	14
1486	1336	1384	18
1470	1236	1322	10
1500	1260	1358	18
1436	1182	1324	32
1418	1212	1250	28

Table 1: Coincidence counts for different angle configurations of the measurement HWPs. Notice the similar values in $N(0°, 0°), N(45°, 45°)$ and $N(90°, 90°)$, which is behavior we expect.

match exactly what the mathematics tell us. For a perfect bell state, we have $\theta = 45°$ and $\delta = 0$, so $P_{vv}(\alpha, \beta)$ has a very nice interpretation:

$$P_{vv}(\alpha, \beta) = \frac{1}{2}\cos^2(\beta - \alpha)$$

meaning that the probability only depends on the difference between the two angles. Because the phase δ doesn't change in our experiment, then this means that regardless of the value of δ, the probability should be constant and only a function of the difference $\beta - \alpha$. In the context of our data, this means that $N(0°, 0°), N(45°, 45°)$ and $N(90°, 90°)$ should all have similar values, and this is precisely what we see in table [1].

5.2 Calculating S

With the Bell state characterized, we are ready to move on to the final quantity to calculate, which is to calculate S. Recall that earlier we introduced the CHSH inequality as the quantity S:

$$S = E(\alpha, \beta) - E(\alpha, \beta') + E(\alpha', \beta) + E(\alpha', \beta') \leq 2$$

where each $E(\alpha, \beta)$ is defined as:

$$E(\alpha, \beta) = \frac{N_{vv} + N_{vh} - N_{hv} + N_{hh}}{N_{\text{total}}}$$

So, now we define a measurement basis that maximizes S. It should be noted that we need to be specific about which basis we choose, as not all $\alpha, \alpha', \beta, \beta'$ values will violate $|S| \leq 2$. Following [1], we choose our angles $\alpha = 0°, \beta = 22.5°$, and $\alpha' = 45°, \beta' = 67.5°$ and measure the coincidence counts for each pair $(\alpha, \beta), (\alpha', \beta), (\alpha, \beta'), (\alpha', \beta')$, which is summarized in table 2. As for the uncertainties in our measured coincidences, we can derive the uncertainty by using the fact that the coincidence counting is a Poisson process, and thus the variance scales with $\sqrt{N}$, where N is the count.

From here, it is easy to calculate S, which we can compute by simply calculating $E(\alpha, \beta)$ for each pair of angles, and sum them all to get S. For our data, we obtain a value of $S = 2.52 \pm 0.07 > 2$, so the CHSH inequality is violated. This allow us to conclude that hidden variable theories cannot be at play, since had they existed the value of S would be bounded. This is the ultimate result that we want to achieve, so this result concludes the experiment.

6 Conclusion and Reflection

Overall, with the CHSH inequality violated, this indicates that our experiment was indeed successful in demonstrating that there are no hidden variable theories at play. In truth, while reproducing such a famous result in the lab is certainly rewarding,

Angle pairs	Polarization A	Polarization B	Coincidences
(α, β)	0	22.5	1323.8
	90	22.5	268.8
	90	112.5	1251.4
	0	112.5	321.2
(α, β')	0	67.5	190.2
	90	67.5	1341.6
	90	157.5	186.4
	0	157.5	1434.2
(α', β)	45	22.5	1319.2
	135	22.5	334.4
	135	112.5	1229.4
	45	112.5	268.8
(α', β')	45	67.5	1237.0
	135	67.5	414.2
	135	157.5	1244.4
	45	157.5	373.2

Table 2: Collected coincidences for the (α, β) pairs described, which is then used to compute S. For each coincidence we have, as it is modeled by a Poisson process, has an uncertainty of $\sqrt{N}$, where N is the number of coincidences we have.

this lab certainly felt more frustrating than enjoyable at times particularly due to the amount of time we had to spend calibrating the device. Because of all the degrees of freedom we had to control, at times it felt like there were so many variables we had to keep track of that troubleshooting the source of an error was an immense challenge.

All in all, this lab really gave me a newfound respect for all the experimentation labs out there that use lasers and complex optical setups. In this context, our experimental setup is extremely simple: one laser, a couple of half wave plates and a detector is all that there is, and even such a simple setup took us *days* to calibrate properly before we could measure a result. It really puts into context why these experiments are so sensitive to small deviations, and I can only imagine how difficult it is to "debug" the experiment.

Despite all this though, there are still some very fun parts of the lab that I take away: this was my first time working with a laser of this power which felt very cool, and also learning of the creative ways we calibrate our instruments (such as sending the red laser backwards through the detector and aiming it to align the beam path) was very interesting – it makes me want to learn more about how calibration of larger setups are conducted.

References

[1] Dietrich Dehlinger and M. W. Mitchell. "Entangled Photons, Nonlocality, and Bell Inequalities in the Undergraduate Laboratory". In: *American Journal of Physics* 70.9 (Sept. 1, 2002), pp. 903–910. ISSN: 0002-9505, 1943-2909. DOI: 10.1119/1.1498860. URL: https://pubs.aip.org/ajp/article/70/9/903/1055905/Entangled-photons-nonlocality-and-Bell (visited on 12/17/2024).

[2] cvimellesgriot. *Fundamental Optics.*

[3] Physics 111B: Advanced Experimentation Laboratory. *Quantum Interference & Entanglement.*